Bakheet et al. Journal of Analytical Science and Technology (2016) 7:4
DOI 10.1186/s40543-016-0082-9

Journal of Analytical Science and Technology
a SpringerOpen Journal

RESEARCH ARTICLE Open Access

New magnetic solid phase extractor based on ionic liquid modified β-cyclodextrin polymer/Fe_3O_4 nanocomposites for selective separation and determination of linuron

Almojtaba Bakheet, Jie Liu and Xiashi Zhu*

Abstract

Background: Direct determination of trace analyte, in particular at ultra-trace concentration, cannot be easily achieved in complex systems by UV-visible spectrometry because of the lack of sensitivity and selectivity of the method. Therefore, an efficient separation step is often required prior to the determination. In accordance, a new magnetic solid phase extractor based on ionic liquid modified carboxymethyl-hydroxypropyl-β-cyclodextrin polymer magnetic particles Fe_3O_4 functionalized with ionic liquid (IL-CM-HP-β-CDCP magnetic nanoparticles (MNPs)) was developed for a selective separation of linuron prior to its determination by UV-visible spectrometry.

Methods: Ionic liquid modified carboxymethyl-hydroxypropyl-β-cyclodextrin polymer magnetic particles Fe_3O_4 (Fe_3O_4@IL-CM-HP-β-CDCP) were confirmed by Fourier transform infrared spectroscopy, scanning electron microscopy, and X-ray powder diffraction (XRD). The uptake behavior of the new Fe_3O_4@IL-CM-HP-β-CDCP MNPs adsorbent toward linuron was studied. The concentrations of linuron were directly determined after reading absorbance by UV-visible spectrometry.

Results: Fourier transform infrared spectroscopy, scanning electron microscopy, and XRD results strongly confirmed the formation of Fe_3O_4@IL-CM-HP-β-CDCP MNPs phase. Adsorption study revealed the Fe_3O_4@IL-CM-HP-β-CDCP MNPs for a selective separation of linuron prior to its determination by UV-visible spectrometry. The results showed that linuron was adsorbed rapidly on Fe_3O_4@IL-CM-HP-β-CDCP MNPs and eluted by 4.0 mL ethanol in 15 min. Under the optimized conditions, the linear calibration curves for linuron were obtained over the concentration range of 0.07–19.00 μg mL^{-1} with a relative standard deviation of 1.97 % ($n = 3$, $c = 4.00$ μg mL^{-1}). The detection limits, the limit of quantification, correlation coefficient (R), and preconcentration factor were 7.0 μg L^{-1}, 70.0 μg L^{-1}, 0.9987, and 15, respectively.

Conclusions: Ultimately, the developed method can be applied and effectively utilized for the determination of linuron in real samples.

Keywords: Linuron, Ionic liquid, Nanocomposites, Magnetic solid phase extraction, UV-visible spectroscopy

* Correspondence: xszhu@yzu.edu.cn
College of Chemistry & Chemical Engineering, Yangzhou University, Yangzhou 225002, People's Republic of China

Background

Linuron (Fig. 1) is one of the urea herbicides; it was developed by the DuPont as urea herbicides in 1960 and was widely used in agricultural production (Lima et al. 2011). But, it could exist in environment stably for a long time and thus pollute the soil and surface water, seriously damaging the groundwater and organisms (Ornostay et al. 2013). Toxicological studies indicated that these herbicides have different degrees of toxicity on humans and even have carcinogenic effects (Daam et al. 2009). Therefore, the accurate, sensitive, and at the same time quick and easy detection of linuron residues in fruits and vegetables is a method of great significance.

Various methods have been developed for the determination of linuron to date, including HPLC (Katsumata et al. 2007), electrochemical method (Lima et al. 2011), HPLC-MS (Petrovic et al. 2010), sensor method (Ciumasu et al. 2005), capillary electrophoresis (Da Silva et al. 2003), and UV spectrometry (Chen and Zhu 2015). UV spectrometry has many advantages including simple operation, lower cost, and repeatable results. However, the direct determination with spectrophotometry for linuron is difficult owing to matrix effects and its lower concentration in natural samples. So, UV spectrometry is often combined with separation/enrichment technique to improve the selectivity and sensitivity of detection (Chen and Zhu 2015).

Magnetic solid phase extraction (MSPE) is a kind of magnetic or magnetizable material as absorbent matrix solid phase extraction technique (Giakisikli and Anthemidis 2013), which has many advantages including simple operation, short extraction time, low organic solvent consumption, and easy automation. It has a broad application prospect in detection analysis (Jiang et al. 2013). To date, MSPE extraction agent is mainly Fe_3O_4 nanoparticles (NPs) with specific chemical functional group modified on the surface to achieve concentration of the targeted analytes. Numerous organic polymers and inorganic polymers have been used to modify Fe_3O_4 NPs. The unique structures of cyclodextrins (CDs), which have a cavity possessing a hydrophilic external surface and a hydrophobic internal surface, make them useful in separation processes. β-CDCP by polymerizing cyclodextrin with epichlorohydrin was a spherical or grainy solid subject and insoluble in water, which still retained the inclusion property of β-CD, was synthesized by the reaction of β-CD and cross-linked agent. β-CDCP as a solid phase extraction material had been applied to selectively separation/preconcentration the similar size of materials (Zhu and Ping 2014). Yu et al. modified the Fe_3O_4 NPs with hydroxypropyl-β-cyclodextrin (HP-β-CD) and polyethyleneglycol 400 (PEG400) for the removal of congo red from aqueous solutions (Yu et al. 2014). The related research by our group indicated (1) Fe_3O_4@cyclodextrin polymer NPs (Fe_3O_4@β-CDCP) as adsorbents for preconcentration/extraction of rutin from lotus plumule (Gong et al. 2014) and (2) self-assembly Fe_3O_4@SiO_2@ILs as adsorbents for preconcentration/extraction of linuron (Chen and Zhu 2015). But, there was no report to separation/analysis linuron with Fe_3O_4@IL-CM-HP-β-CDCP magnetic nanoparticles (MNPs).

In this study, carboxymethyl-hydroxypropyl-β-cyclodextrin polymer magnetic particles Fe_3O_4 (Fe_3O_4@CM-HP-β-CDCP) which has a good hydrophobic and stability properties were prepared and modified with ionic liquid (Fe_3O_4@IL-CM-HP-β-CDCP). The magnetic solid phase extraction followed by UV-vis spectroscopy was applied to separation/analysis linuron in real samples with reasonable results. Compared with the previously reported works, (1) this adsorbent-based MSPE provides a rapid and efficient sample preparation process, which enables the treatment of large volume samples in a short period of time (Gong et al. 2014; Cheng et al. 2012) and (2) the adsorbent Fe_3O_4@IL-CM-HP-β-CDCP MNPs could be used repeatedly and better preconcentration factor (Chen and Zhu 2015).

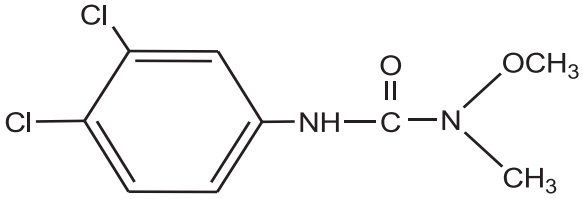

Fig. 1 Chemical structure of linuron

Methods

Materials and reagents

Fourier transform infrared spectroscopy (FTIR) spectra were measured with a Bruker Tensor 27 spectrometer

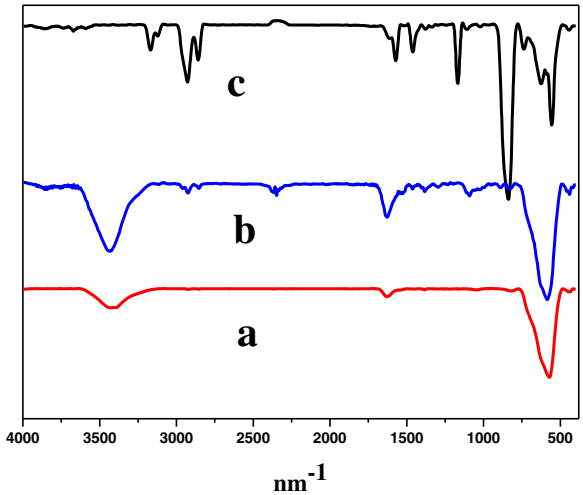

Fig. 2 Infrared spectra. **a** Fe_3O_4. **b** Fe_3O_4@CM-HP-β-CDCP. **c** Fe_3O_4@IL-CM-HP-β-CDCP

(Bruker Company, Germany). Samples were pressed into KBr pellets and recorded at the frequencies from 4000 to 400 cm^{-1} with resolution of 4 cm^{-1}. A SEM Hitachi S-4800 II instrument was used to obtain micrographs of the material. UV-2500 spectrophotometer (Shimadzu Corporation, Japan) was used. Neodymium magnet and timing multifunctional oscillator (Guohua Limited Company, China), a digital water-bath (Guohua Limited Company, China), and pH meter (Shanghai Jinke Limited Company, China) were used.

All chemicals and reagents were at least of analytical reagent grade, unless otherwise stated, as follows: *N*-methylimidazole (Darui Fine Chemicals, Shanghai, China), 1-bromooctane (Sinopharm Chemical Reagent Co., Ltd., Shanghai, China), KPF_6, $FeCl_3$, $FeSO_4 \cdot 7H_2O$, acetone, methylene chloride, NaOH, HCl, carbinol, ethanol, sodium dodecyl sulfate (SDS), acetonitrile (ACN), hydroxypropyl-β-cyclodextrin, and epichlorohydrin (Shanghai Chemical Reagent Corporation, China). Linuron standards were obtained from the Sigma-Aldrich (Shanghai, China). A standard stock solution was prepared by dissolving 10.0 mg of each standard in 100 mL of ethanol and stored in dark at 4 °C. Working standard solutions were obtained by appropriate dilution of the stock solution.

Experiment method

Synthesis of Fe_3O_4@IL-CM-HP-β-CDCP MNPs

Synthesis of CM-HP-β-CDCP MNPs CM-HP-β-CDCP MNPs were prepared according to literature (Badruddoza et al. 2013).

Synthesis of Fe_3O_4@IL-CM-HP-β-CDCP MNPs $[C_8MIM][PF_6]$ was synthesized according to literature (Zhao et al. 2007). Then, 5 g of CM-HP-β-CD polymer was stirred for 3 days in 20 mL of $[C_8MIM][PF_6]$ medium for effective impregnation. The adsorbent was dried at 90 °C for 3 days. Then, the product was dried at 90 °C for 24 h and sonicated for 1 day again, and the resulting polymer was Fe_3O_4@IL-CM-HP-β-CDCP MNPs.

Sample preparation

Water sample: Lake water was collected from the Slender West Lake in Yangzhou, China. A 50.0 mL of lake water sample was filtered through a 0.45-μm membrane to remove suspended particles before analysis.

Fruit and vegetable samples (Farokhcheh and Alizadeh 2013): Apple and lettuce samples were supplied by our local market. A 20.0 g of apple (or lettuce) slurry and 20 mL anhydrous ethanol were placed in a 50-mL centrifuge, and the mixture was then shaken for 20 min. After centrifugation, the upper fluids in the tube were filtered and collected in a volumetric flask.

Procedure of adsorption and elution

A 40.0 mL of the working solution or aqueous sample and 0.10 g of Fe_3O_4@IL-CM-HP-β-CDCP MNPs were transferred into a centrifuge tube, and the solution in the tube was subsequently shaken in the constant temperature shaking table for 20 min at room temperature. Then, Fe_3O_4@IL-CM-HP-β-CDCP MNPs with adsorbed target linuron was separated from the solution by an external magnetic field. The residual linuron in the supernatants was determined by UV-vis spectroscopy at 246 nm.

In the adsorption of linuron Fe_3O_4@IL-CM-HP-β-CDCP MNPs with 4.0 mL ethanol ultrasound elution for 20 min, eluent were determined by the UV-vis spectroscopy.

Determination of inclusion constant

The procedure of the determination of inclusion constant was based on the literature (Zhou et al. 2013).

Results and discussion

Characterization of Fe_3O_4@CM-HP-β-CDCP MNPs

Characterization by FTIR

Figure 2 shows the FTIR spectra of Fe_3O_4 (curve a), Fe_3O_4@CM-HP-β-CDCP MNPs (curve b), and Fe_3O_4@IL-CM-HP-β-CDCP MNPs (curve c) in the range of 4000–400 cm^{-1} wave number range. The results are as follows: (1) the peak of 580 cm^{-1} showed was assigned to Fe-O-Fe stretching vibration (curve a and b), the peak of 2400 and 2850 cm^{-1} on curve b corresponded to the C-H stretching vibration in CM-HP-β-CDCP, and the peaks at 1628 cm^{-1} on curve b was stronger than on curve a, which illustrated that CM-HP-β-CD was coated Fe_3O_4 surface (curve a and b); (2) in the curve c, the peaks at 3171 and 3125 cm^{-1} embody the spectrum of the C-H stretching vibration, the peaks at 1573 and 1462 cm^{-1} corresponded to the characteristic absorption of imidazole groups, and 739 cm^{-1} corresponded to long chain CH_2; moreover, the peak of 840 cm^{-1} was attributed to the P-F stretching vibration. These results confirm that IL had been successfully immobilized on the surface of Fe_3O_4@CM-HP-β-CDCP MNPs (curve b and c).

Characterization by SEM

The morphological structures of Fe_3O_4(A), Fe_3O_4@CM-HP-β-CDCP(B), and Fe_3O_4@IL-CM-HP-β-CDCP(C) were investigated with the scanning electron micrographics showed in Fig. 4. It could be seen that (1) the globular apparent structure was not changed after CM-HP-β-CD coated on Fe_3O_4 (Fig. 4a, b) and (2) the morphology of Fe_3O_4@IL-CM-HP-β-CDCP MNPs was distinctly different (Fig. 4c), which showed the presence of ionic liquid. Therefore, together with the results of FT-IR, the

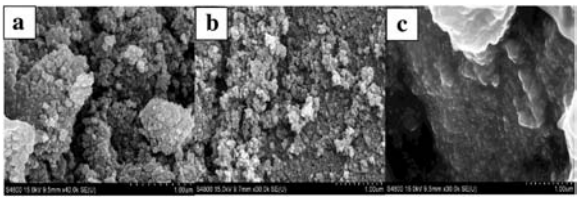

Fig. 3 SEM image. **a** Fe_3O_4. **b** Fe_3O_4@CM-HP-β-CDCP. **c** Fe_3O_4@IL-CM-HP-β-CDCP

Fe_3O_4@CM-HP-β-CDCP MNPs were successfully coated by $[C_8MIM][PF_6]$ (Fig. 3).

Characterization by XRD

X-ray powder diffraction (XRD) measurements were carried out to investigate the phase structure of the obtained samples. The XRD pattern of Fe_3O_4 (curve a), Fe_3O_4@CM-HP-β-CDCP MNPs (curve b), and Fe_3O_4@IL-CM-HP-β-CDCP MNPs (curve c) were shown in Fig. 4. Six characteristic diffraction peaks of Fe_3O_4 could be found at $2\theta = 30.1°$, 35.4°, 43.1°, 53.4°, 57.2°, and 62.5°; these could be assigned to diffractions from the (220), (311), (400), (422), (511), and (440) planes of Fe_3O_4, respectively, indicating that modification of the MNP surface with CM-HP-β-CD and IL did not change the phase of Fe_3O_4, but the peaks of Fe_3O_4@IL-CM-HP-β-CDCP MNPs became weaker than naked Fe_3O_4.

Magnetization curves

The magnetic properties of magnetic absorbents directly influence recovery efficiency. In this study, VSM was used to estimate the magnetic properties of the prepared nanocomposite at room temperature. Figure 5 shows the hysteresis loops for the material (a) Fe_3O_4, (b) Fe_3O_4@CM-HP-β-CDCP MNPs, and (c) Fe_3O_4@IL-CM-HP-β-CDCP MNPs. The maximal saturation magnetization of Fe_3O_4(-curve a) was 48 emu g^{-1}; after modified with CM-HP-β-CD and IL-CM-HP-β-CD, the maximal saturation magnetizations decreased to 31 and 21 emu g^{-1}, respectively. It may be caused by the nonmagnetic of CM-HP-β-CD and IL-CM-HP-β-CD. The saturation magnetization of 16.3 emu g^{-1} was sufficient for magnetic separation with a magnet (Caruntu et al. 2004). Therefore, the IL-CM-HP-β-CD MNPs prepared here could be rapidly separated from solution with a magnet on the account of their superparamagnetism and large saturation magnetization.

Optimization of adsorption

Effect of pH

The effect of pH was investigated by varying the pH values between 3.0 and 9.0 (Fig. 6). The results depicted that (1) the adsorption behavior of linuron on Fe_3O_4@CM-HP-β-CDCP MNPs (curve a) and Fe_3O_4@IL-CM-HP-β-CDCP MNPs (curve b) was similar, the adsorption efficiency of linuron on Fe_3O_4@CM-HP-β-CDCP MNPs(E_1) was lesser than that on Fe_3O_4@IL-CM-HP-β-CDCP MNPs(E_2), and linuron could only quantitatively be absorbed on Fe_3O_4@IL-CM-HP-β-CDCP MNPs. It may be caused by the effect of IL on the Fe_3O_4@CM-HP-β-CDCPMNPs about its hydrophobicity (Ma et al. 2005); (2) linuron could be quantitatively absorbed on Fe_3O_4@IL-CM-HP-β-CDCP MNPs in the test pH range, and maximum at pH = 7.0, which showed that the adsorption efficiency of linuron was not affected by pH. Thus, all subsequent studies were performed in pH 4.0–7.0.

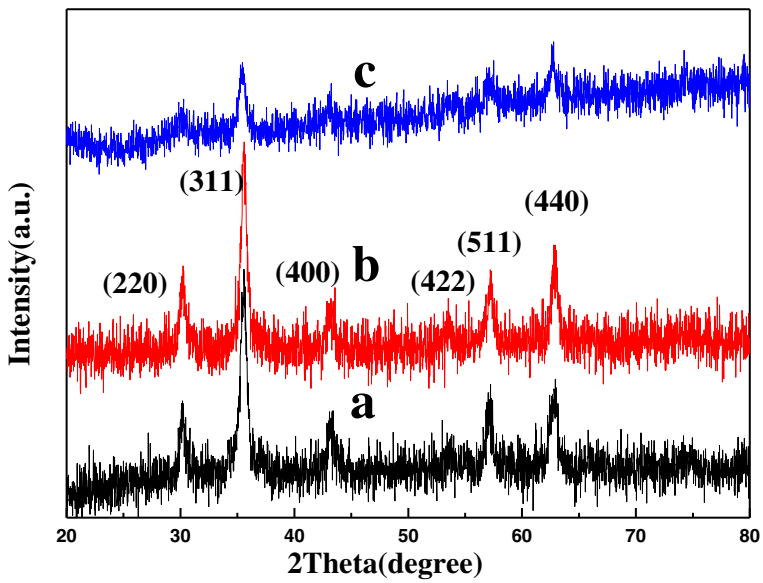

Fig. 4 XRD patterns. **a** Fe_3O_4. **b** CM-HP-β-CD MNPs. **c** IL-CM-HP-β-CD MNPs

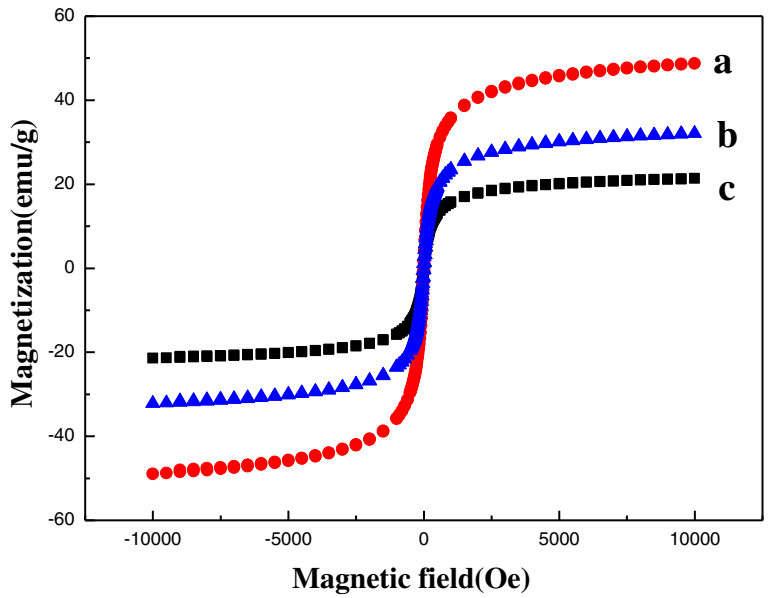

Fig. 5 Magnetic hysteresis loops. **a** Fe_3O_4. **b** Fe_3O_4@CM-HP-β-CDCP. **c** Fe_3O_4@ IL-CM-HP-β-CDCP

Effect of adsorption temperature

The effect of temperature (10.0 °C 50.0 °C) on the adsorption efficiency of linuron was tested. Linuron could effectively be absorbed on the Fe_3O_4@IL-CM-HP-β-CDCP MNPs in the range of 20–40 °C; herein, the adsorption of the analyte was conveniently carried out at room temperature.

Effect of adsorption time

The effect of adsorption time on the adsorption efficiency was carefully studied in the range from 5–60 min. The results illustrated that adsorption efficiency of linuron finished after 20 min and stabled. Thereafter, 20 min of extraction time was performed for further study.

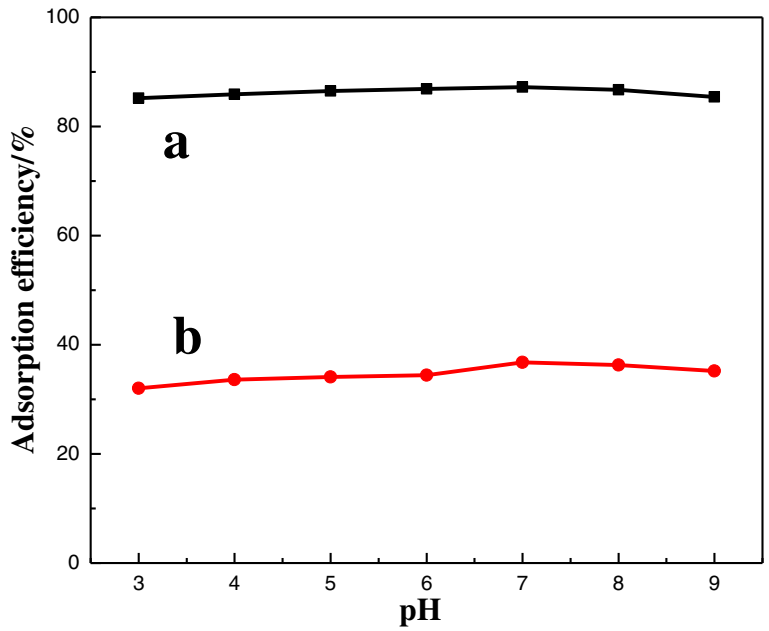

Fig. 6 Effect of pH on the adsorption efficiency. **a** Fe_3O_4@CM-HP-β-CDCP MNPs. **b** Fe_3O_4@IL-CM-HP-β-CDCP MNPs

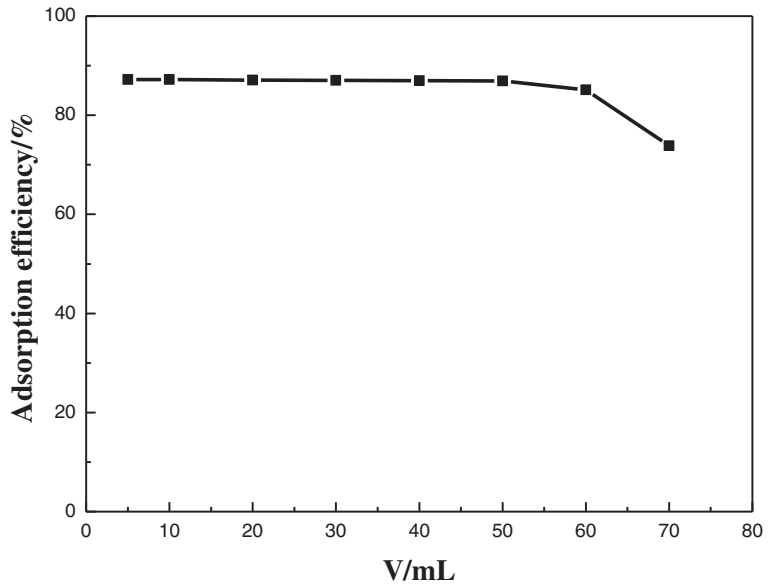

Fig. 7 Effect of sample volume on the adsorption efficiency

Effect of sample volume

The concentration of linuron was fixed at 4.0 μg mL^{-1}, and the volume of the sample solution was increased from 5.0 to 70.0 mL. It could be seen in Fig. 7 that the adsorption efficiency was greater than 85.0 % in the sample volume of 5.0–60.0 mL and decreased when the sample volume was greater than 60.0 mL, so the allowed sample volume was 60.0 mL.

Adsorption capacity

Adsorption capacity is defined as the maximum amount of analyte adsorbed per gram of Fe_3O_4@IL-CM-HP-β-CDCP MNPs. The adsorption capacity (qe in mg g^{-1}) of linuron was calculated based on the difference in the linuron concentration in the solution before and after adsorption (Akkaya 2013), according to the following equation:

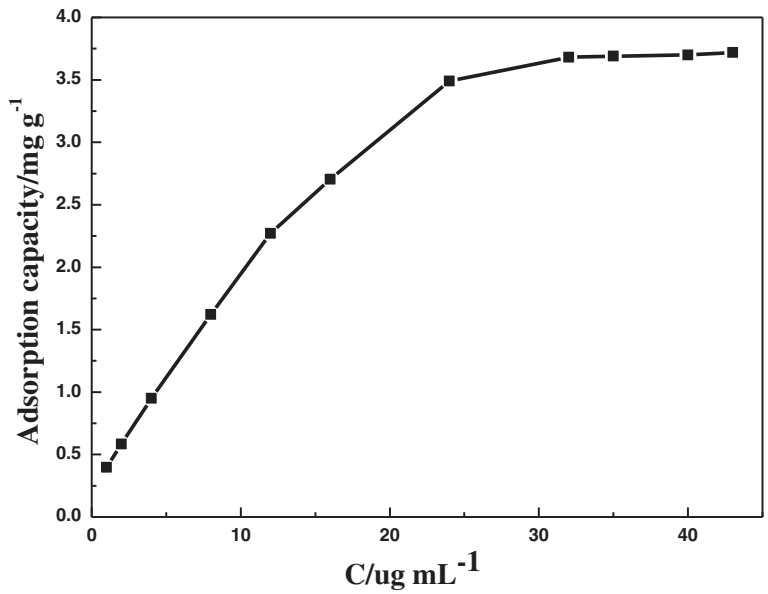

Fig. 8 Adsorption capacity

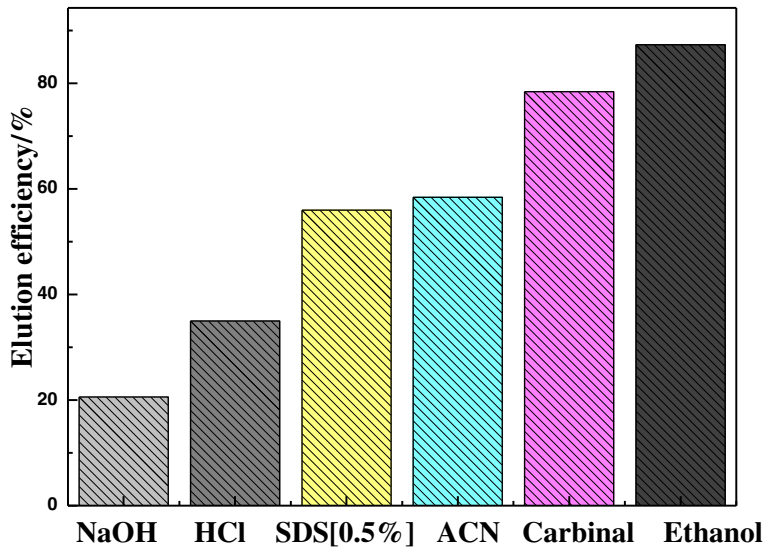

Fig. 9 Effect of different dissolvent on the elution efficiency

$$q_e = \frac{(Co - Ce) \times V}{m}$$

where C_o and C_e are the initial and equilibrium concentration of linuron (μg mL^{-1}), m is the weight of Fe_3O_4@IL-CM-HP-β-CDCP (g), and V is the volume of solution (mL).

Figure 8 indicates that the adsorption of linuron reached the maximum when the concentration was 43.00 μg mL^{-1}; the adsorption capacity for Fe_3O_4@IL-CM-HP-β-CDCP MNPs was calculated finally as 3.72 mg g^{-1}.

Optimization of elution

Selection of eluent

The selection of eluent type is of vital importance which determines the final extraction efficiency. Therefore, several eluent (0.1 mol/L HCl, NaOH, 0.5 % SDS, ACN, carbinol, ethanol) were tested in this work. As can be seen from Fig. 9, the ethanol had the strongest elution capacity for linuron. Thus, ethanol was chosen as the final eluent.

Effect of elution temperature

The elution efficiency of linuron at different temperatures (10–50 °C) was studied. The elution efficiency

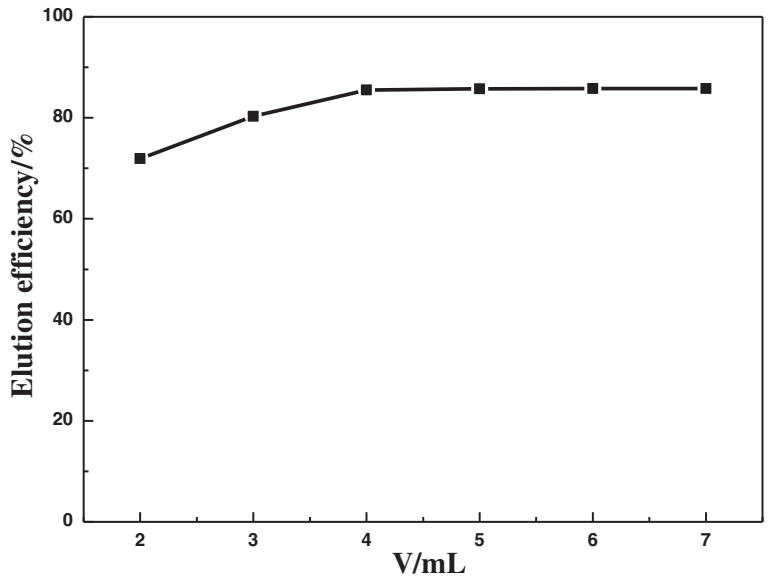

Fig. 10 Effect of volume on the elution efficiency

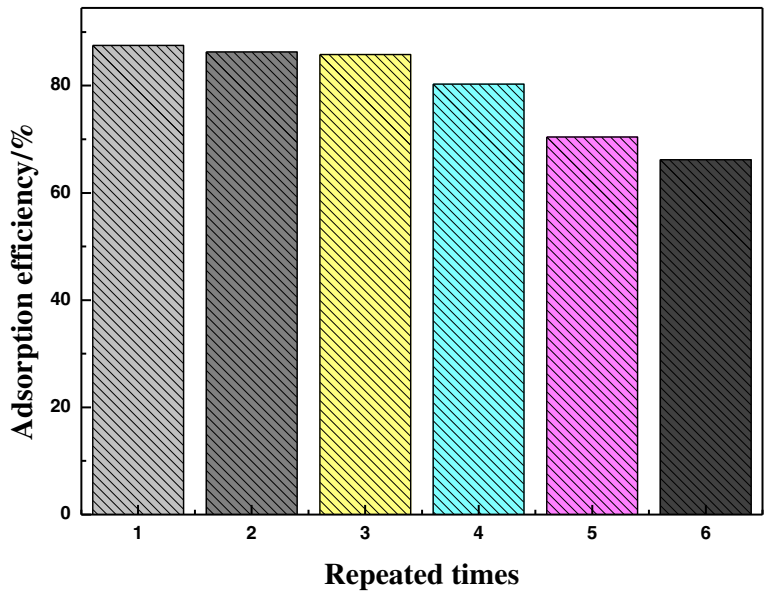

Fig. 11 Repeated times

increased progressively with the temperature from 5 to 20 °C. And, the elution efficiency of linuron was greater than 85.0 % and remained constant at the elution temperature ranging from 20 to 40 °C. Accordingly, the elution was performed at room temperature.

Effect of elution time

The effect of elution time on the elution of linuron was also estimated. The elution efficiency of linuron became stable after 15 min. Thereafter, 15 min of elution time was selected for further studies.

Effect of eluent volume

Then, elution efficiency of linuron with 2.0–7.0 mL of ethanol was studied (Fig. 10). The elution efficiencies of linuron was above 85 % from 4.0 to 7.0 mL and reached the biggest in 4.0 mL. The preconcentration factor is 15 (the quotient of volume before absorption and after elution). Therefore, the optimum volume of ethanol solution chosen for this work was 4.0 mL.

Table 1 Tolerance of interference ions

Interference	Tolerance ratio in mass (*w/w*) (tested substances to analyte ratio)
Zn^{2+}	200
Cu^{2+}, tebuconazole	40
Triadimefon, 2-nitrophenol	20
Fe^{3+}, NO_3^-, SO_4^{2-}	15
Carbendazim, benomyl, acetamiprid	15
4-Nitrophenol, phenol	15
Diuron	5

Reuse of Fe_3O_4@IL-CM-HP-β-CDCP MNPs

The reusability of IL-CM-HP-β-CDCP MNPs was evaluated through consecutive adsorption and elution cycles. As shown in Fig. 11, the IL-CM-HP-β-CDCP MNPs could be reused at least five times along with the adsorption efficiency of above 85.0 % for linuron.

Effect of interference

Determination of linuron (5.00 μg L^{-1}) in the presence of foreign substances was investigated. With a relative error less than ±5 %, the tolerance limits for various foreign substances are listed in Table 1 (tolerance ratio in mass). The results indicated that the majority of these

Table 2 The recoveries of linuron in samples ($n = 3$)

Sample	Added (μg/mL)	Found (μg/mL)	Recovery (%)
Lake water	0.00	ND	–
	0.50	0.48	96.0
	4.00	3.93	98.3
	8.00	7.91	98.9
Lettuce	0.00	ND	–
	0.50	0.49	98.0
	4.00	3.98	99.5
	8.00	8.05	100.6
Apple	0.00	ND	–
	0.50	0.48	96.0
	4.00	3.96	99.0
	8.00	7.94	99.3

ND No detection

substances in samples had no remarkable interference on the linuron determination.

Analytical performance of the method

Once optimized, the method was finally characterized in terms of linearity, precision, accuracy, and sensitivity. Under the optimum conditions, the matrix matching calibration curve of noninterference was established with standard addition method in the concentration range of 0.07–19.0 μg mL^{-1}. The equation of calibration graph was $A = 0.231c + 0.057$ (μg mL^{-1}), with a correlation coefficient of 0.9987. The limit of detection, defined as LOD = 3 σ/k (where σ is the standard deviation of blank and k is the slope of calibration graph) was 7.0 μg L^{-1}. The limit of quantification was 70.0 μg L^{-1}. The precision (relative standard deviation) was 1.97 % ($n = 3$, $c = 4.00$ μg mL^{-1}). The preconcentration factor, defined as the quotient of volume before absorption and after elution, was 15-fold.

Sample analysis

Under the optimum conditions, the proposed method was applied to determine linuron in lake water, lettuce, and apple samples. Since no positive samples were found, a recovery study was performed using the standard addition method with the analyte at three different concentrations (12.5, 25.00, and 125.0 μg kg^{-1}). The data, which is summarized in Table 2, showed the accuracy (excellent recovery values) in all instances, and the proposed methodology was suitable for the determination of linuron.

Comparison with other methods

Compared to other methods, it is obvious that the present work has low detection limit and wide linear range (Table 3). Moreover, the proposed method has advantages of simple operation and lower analysis cost.

Discussion of extraction mechanism

The inclusion constant K is a significant parameter which illustrates inclusion interactions of host-guest molecules. The inclusion complex can be easily formed at a higher K. The inclusion constants of the monomers of two kinds of polymers (CM-HP-β-CD and IL-CM-HP-β-CD) and linuron were measured. The form of inclusion and the inclusion constant can be calculated by UV-visible absorption spectroscopy and Hildebrr and Benesi equation (Zhao et al. 2007).

Table 3 Comparison with the results in other literatures

Method	Linear range (μg mL^{-1})	Limit of detection (μg L^{-1})	Ref.
SPE/HPLC	–	50.0	Zhao et al. 2004
MSPD/RP-HPLC	0.025–10.00	10.0	Xiao et al. 2010
Micro extraction bottles enrichment/ HPLC	0.06–6.00	5.0	Li et al. 2013
MSPE/UV	0.04–20.00	5.0	Chen and Zhu 2015
MSPE/UV	0.07–19.00	7.0	The proposed method

The double reciprocal plots of the (CM-HP-β-CD)-linuron inclusion complex (A) and (IL-CM-HP-β-CD)-linuron inclusion complex (B) are shown in Fig. 12. It can be concluded that (1) the two double reciprocal plots show good linearity with correlation coefficients of 0.9961 for CM-HP-β-CD (Fig. 12a) and 0.9844 for CM-HP-β-CD-IL (Fig. 12b), which illustrated that both CM-HP-β-CD and IL-CM-HP-β-CD form the inclusion complexes with linuron at a ratio of 1:1 and (2) the inclusion constant of CM-HP-β-CD-linuron inclusion complex and for IL-CM-HP-β-CD-linuron inclusion complex is K_1 1.08×10^3 and K_2 1.35×10^3 L/mol, respectively, which are acquired by the slope and intercept of the double reciprocal plots. On the basis of the inclusion constant, we could get the following conclusion: (1) Inclusion constant reflects the inclusion ability of a host molecule to a guest molecule. $K_2 > K_1$, which is consistent with the adsorption efficiency of linuron ($E_2 > E_1$) (Fig. 6), demonstrated that the inclusion ability of IL-CM-HP-β-CD toward linuron is stronger

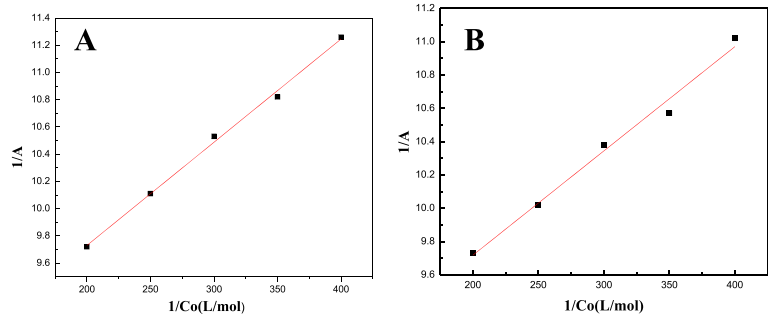

Fig. 12 Double reciprocal plot of the CM-HP-β-CD-linuron inclusion complex (**a**) and the (IL + CM-HP-β-CD)-linuron inclusion complex (**b**). The *error bars* represent standard deviation ($n = 3$)

than of CM-HP-β-CD. That is one reason why IL-CM-HP-β-CD has a higher adsorption efficiency than CM-HP-β-CD; (2) the difference value of K between K_1 and K_2 is not large, but the adsorption efficiency is obviously improved ($E_2 >> E_1$) (Fig. 6). It is mainly because the hydrophobic IL in Fe_3O_4@IL-CM-HP-β-CDCP MNPs is good for the adsorption to hydrophobic pesticides linuron.

Conclusions

Fe_3O_4@IL-CM-HP-β-CDCP MNPs used as a solid phase extraction material to preconcentrate/separate linuron coupled with UV for the analysis of linuron is established. The proposed method has some advantages, such as easy, safe, and inexpensive methodology for the separation/determination of linuron in fruit and vegetable samples.

Competing interests

The authors declare that they have no competing interests.

Authors' contributions

XSZ designed the experiment and revised the manuscript. Experimental part and manuscript were carried out by AB, JL and XSZ is the corresponding author. All the authors have read and approved the final manuscript.

Acknowledgements

The authors acknowledge the financial support from the National Natural Science Foundation of China (21375117) and a project funded by the Priority Academic Program Development of Jiangsu Higher Education Institutions.

Received: 3 October 2015 Accepted: 11 January 2016

References

Akkaya R. Removal of radioactive elements from aqueous solutions by adsorption onto polyacrylamide-expanded perlite: equilibrium, kinetic, and thermodynamic study. Desalination. 2013;321:3–8.

Badruddoza AZM, Shawon ZBZ, Daniel TWJ, Hidajat K, Uddin MS. Fe_3O_4/cyclodextrin polymer nanocomposites for selective heavy metals removal from industrial wastewater. Carbohydr Polym. 2013;91:322–32.

Caruntu D, Caruntu G, Chen YX, O'Connor CJ, Goloverd G, Kolesnichenko VL. Synthesis of variable-sized nanocrystals of Fe_3O_4 with high surface reactivity. J Mater Chem. 2004;16:5527–34.

Chen JP, Zhu XS. Ionic liquid coated magnetic core/shell Fe_3O_4@SiO_2 nanoparticles for the separation/analysis of linuron in food samples. Spectrochim Acta A. 2015;137:456–62.

Cheng Q, Qu F, Li NB, Luo HQ. Mixed hemimicelles solid-phase extraction of chlorophenols in environmental water samples with 1-hexadecyl-3-methylimidazolium bromide-coated Fe_3O_4 magnetic nanoparticles for high-performance liquid chromatographic analysis. Anal Chim Acta. 2012;715:113–9.

Ciumasu IM, Kramer PM, Weber CM, Kolb G, Tiemann D, Windisch S, et al. A new, versatile field immunosensor for environmental pollutants: development and proof of principle with TNT, diuron, and atrazine. Biosens Bioelectron. 2005;21:354–64.

Da Silva CL, De Lima EC, Tavares MFM. Investigation of preconcentration strategies for the trace analysis of multi-residue pesticides in real samples by capillary electrophoresis. J Chromatogr A. 2003;1014:109–16.

Daam MA, Rodrigues AMF, Van den Brink PJ, Nogueira AJA. Ecological effects of the herbicide linuron in tropical freshwater microcosms. Ecotoxicol Environ Saf. 2009;72:410–23.

Farokhcheh A, Alizadeh N. Determination of diphenylamine residue in fruit samples using spectrofluorimetry and multivariate analysis. LWT Food Sci Technol. 2013;54:6–12.

Giakisikli G, Anthemidis AN. Magnetic materials as sorbents for metal/metalloid preconcentration and/or separation. Anal Chim Acta. 2013;789:1–16.

Gong AQ, Ping WH, Wang J, Zhu XS. Cyclodextrin polymer/Fe_3O_4 nanocomposites as solid phase extraction material coupled with UV–vis spectrometry for the analysis of rutin. Spectrochim Acta A. 2014;122:331–6.

Jiang HM, Yang T, Wang YH, Lian HZ, Hu X. Magnetic solid-phase extraction combined with graphite furnace atomic absorption spectrometry for speciation of Cr(III) and Cr(VI) in environmental waters. Talanta. 2013;116:361–7.

Katsumata H, Asai H, Kaneco S, Suzuki T, Ohta K. Determination of linuron in water samples by high performance liquid chromatography after preconcentration with octadecyl silanized magnetite. Microchem J. 2007;85:285–9.

Li H, Shi LM, Zhou JK. Determination of urea herbicide in tea drinks by microextraction flask-liquid chromatography. Food Ferment Technol. 2013;49:78–81.

Lima F, Gozzi F, Fiorucci AR, CardosoC AL, Arruda GJ, Ferreira VS. Determination of linuron in water and vegetable samples using stripping voltammetry with a carbon paste electrode. Talanta. 2011;83:1763–8.

Ma Z, Guan Y, Liu H. Synthesis and characterization of micron-sized monodisperse superparamagnetic polymer particles with amino groups. J Polym Sci A. 2005;43:3433–9.

Ornostay A, Cowie AM, Hindle M, Baker CJO, Martyniuk CJ. Classifying chemical mode of action using gene networks and machine learning: a case study with the herbicide linuron. Comp Biochem Physiol Part D. 2013;8(4):263–74.

Petrovic T, Dordevic J, Dujakovic N, Kumric K, Vasiljevic T, Lausevic M. Determination of selected pesticides in environmental water by employing liquid-phase microextraction and liquid chromatography-tandem mass spectrometry. Anal Bioanal Chem. 2010;397:2233–43.

Xiao L, Wang YC, Cheng MR. Determination of phenylureas herbicide residues in tea with matrix solid-phase dispersion-RP-HPLC. J Tea Sci. 2010;1:52–6.

Yu L, Xue WH, Cui L, Xing W, Cao XL, Li HY. Use of hydroxypropyl-β-cyclodextrin/polyethylene glycol 400, modified Fe_3O_4 nanoparticles for congo red removal. Int J Biol Macromol. 2014;64:233.

Zhao JY, Xin JH, Guo YN, Cui XJ, Zhang M, Li JC. Determination of three phenylurea herbicides in water using solid phase extraction and high performance liquid chromatography. Chin J Anal Chem. 2004;32:939–42.

Zhao FY, Wang JY, Liu HJ, Liu RJ. Synthesis and properties of a series of room-temperature ionic liquids N-alky-l-N-methylimidazolium hexafluorophosphates. Huaxue Shiji. 2007;4(29):229–31.

Zhou N, Sang RH, Zhu XS. Functionalized β-cyclodextrin polymer solid phase extraction coupled with UV–visible spectrophotometry for analysis of kaempferol in food samples. Food Anal Methods. 2013;7:1256–60.

Zhu XS, Ping WH. Optimization of β-cyclodextrin cross-linked polymer for monitoring of quercetin. Spectrochimica Acta A. 2014;132:38–43.